BMC Plant Biology

RESEARCH

Open Access

Phytic acid is an available phosphorus source for maize plants in juvenile phase belonging to two populations with different breeding backgrounds

Maria Carelli[1*], Federica Terlizzi[1] and Carla Scotti[1]

Abstract

Background Applying animal effluent/digestate to forage crops can improve the sustainability of intensive livestock husbandry. Organic phosphorus (P) forms, in particular phytic acid ($InsP_6$) present in animal effluent/digestate, would benefit from an effective uptake and assimilation by crops thus representing an alternative to mineral P fertilization and controlling P losses in water system. A maize (*Zea mays* L.) traditional Italian population (VA572), bred before the widespread diffusion of crop chemical fertilization, and a modern commercial hybrid (P1547) were used in this study to investigate their ability of growing in soilless medium using phytic acid (Po) *vs* phosphate P (Pi) as P sources in a 28-day experiment. The hypothesis was that the different agronomical context in which the two varieties were selected could have brought to different abilities in exploiting P sources for plant growth.

Results Quantitative and qualitative growth parameters, root enzymatic phosphatase activities and root transcriptome by RNA-seq analysis were analyzed in this study. Both maize populations were able to grow using phytic acid as the sole P source but organic P utilization was less efficient than Pi; a significant root-released phytase activity, induced by the presence of $InsP_6$, was detected in Po treatment.

The RNA-seq analysis showed different expression patterns induced by organic P treatment (Po) in the two populations. The upregulation in Po treatment of a Purple Acid Phosphatase (PAP) gene and of genes involved in inositol transport indicate that both phosphate hydrolysis from $InsP_6$ by root-secreted PAPs and a direct uptake of myo-inositol at various degrees of phosphorylation could be involved in maize phytic acid exploitation. Root system development and the relationship of P sources with other macro and micro nutrient uptake (N, K, metal ions) were also implied in the response to Po treatment.

Conclusions This study indicates that phytic acid is a bioavailable P source for maize seedling growth. A wider mobilization of genes/pathways was induced by Po treatment in VA572 with respect to P1547 hybrid. The physiological responses to Po treatment were similar in both populations but the patterns of genes involved often differed being specific to each one.

Keywords Maize (*Zea mays* L.), Organic P availability, Phytic acid, Root RNA-seq analysis, F1 hybrid, Open pollinated population

*Correspondence:
Maria Carelli
maria.carelli@crea.gov.it

[1] CREA Research Centre for Animal Production and Aquaculture, Lodi, Italy

Background

In intensive livestock husbandry, the sustainable use of animal effluents, either raw or subjected to anaerobic digestion, is regulated by mitigation strategies (e.g. EU Nitrate Directive 91/676/EEC covering about 61% of European agricultural land; limits to P application in EC Member States; cutting of GHG emissions in the EU 2030 Climate and Energy Framework) aimed at controlling the accumulation of surplus nutrients in soils, in particular nitrogen (N) and phosphorus (P), and limiting losses to water and air systems and the resulting environmental pollution [1]. Phosphorus (P), as an essential macronutrient for crop growth and production, is absorbed by plants as phosphate anions ($H_2PO_4^-$, HPO_4^{2-}) from the soil solution depending on the solubilization of mineral phosphates. Organic P (Po) forms must first be mineralized to become available to plants, a process which is mediated by free soil and rhizosphere microflora or by root-associated microflora e.g. arbuscular mycorrhizal fungi [2–4]. Besides, plants itself have evolved strategies to improve Po assimilation implying a wider exploration of the soil via the development of specific root architecture and morphology [5], the release of root exudates [6] and root-excreted enzymes such as phytases and phosphatases. It is likely that such strategies played a specific role in forage crops because of their long-standing association with livestock husbandry. Alfalfa and silage maize are the most important forage crops sustaining two of the main Po Valley (Northern Italy) agri-food supply chains, the Parmigiano-Reggiano and the Grana Padano cheese production, respectively. In this paper, we investigate the maize's ability to use the Po forms present in digestates/animal effluents as a plant key aspect for increasing the fertilization efficiency of raw and processed manures, decreasing its leaching/emissive potential and contribute to making them an effective alternative to the non-renewable mineral phosphate sources.

Phytic acid, i.e. D-*myo*-inositol (1,2,3,4,5,6) hexakisphosphate or $InsP_6$, was chosen as organic P source in the present study, as soil organic P largely comprises (up to 90%) phosphate monoesters, most of which are in the form of phytate [7] and phytate is the main P storage compound in cereal and oil seeds used in livestock feeding. Although inorganic P represented the major component in dairy farm manure (68%, [8]), digestate (80–90%, [9]) and solid fraction of digestate (> 80%, [10]), organic P amounted for 30% in dairy cattle manure [8] and was part of the biologically available P forms representing 30 to 70% of total phosphorus content in digestate solid fraction [9].

Under low P supply, enhanced activity and secretion of phytases/phosphatases were observed from roots of forage grass and legume species [11], cereals [12, 13] and white lupin [14]. However, few genes or candidate genes encoding root-secreted phytases/phosphatases have been identified and characterised till now in white lupin [14], tomato [15], barrel medic [16], common bean [17], tobacco [18], Arabidopsis [19], soybean [20], rice [21] and poplar [22], thus hampering the display of genetic resource investigation and breeding strategies focused at improving the efficiency of organic P use in forage/fodder species. For instance, a possible adaptation pattern of the alfalfa root-secreted phytase *MsPHY1* gene was found, differentiating two ecotypes originated from intensive *vs* extensive cattle farming regions [23]. In maize, many studies investigated the responses of different genotypes to low P (LP) stress to improve crop tolerance to P deficiency [24, 25] and a promotion of root phosphatase and phytase activity was found at low P and N condition [26–28] but none of the maize phosphatases/phytases identified was clearly associated to root secretion and extracellular hydrolysis of organic P forms [29]. As an attempt to fill this gap and to provide a wider view of the response of maize plant to organic *vs* mineral P sources we used an experimental approach based on a direct comparison of phytic acid ($InsP_6$, indicated as Po) *vs* phosphate (Pi) as unique P sources in axenic conditions face to maize plants from germination to 28 days after transplanting (DAT). Two maize populations were chosen expressing different agronomical contexts of cultivation and breeding, i.e. before and after the widespread diffusion of crop chemical fertilization, to assess possible different abilities in exploiting these P sources for plant growth. Thus, the open pollinated Italian population "Nostrano dell'Isola" (VA572), traditionally cultivated in the plain west side Bergamo (Lombardy, Italy) and object of a breeding work around 1920–30 at the Stazione sperimentale di maiscoltura of Bergamo, was used together with the modern commercial hybrid Pioneer 1547 (P1547). Plant growth parameters, P concentration, P uptake and P use efficiency (PUE) in leaves and roots, root phytase activities and root transcriptome by RNA-seq analysis were analyzed in the different P treatments together with a negative control devoid of P sources (noP).

Materials and methods

Plant materials

Two populations were used in this study: a commercial hybrid (Pioneer 1547), with maturity 130 days (FAO class 600) and the open pollinated Italian population "Nostrano dell'Isola" (VA572), with maturity 135–140 days. Seeds of the VA572 population were provided by the Council for Agricultural Research and Economics

(CREA) – Research Centre for Cereal and Industrial Crops of Bergamo (Italy).

Experimental design

Two independent trials per population – A and B for P1547 hybrid; C and D for VA572– were conducted. The experimental design was a completely randomised design with ninety-six boxes (box = experimental unit, Figure S1) for each trial, eight for each combination P treatment x sampling time. The experimental units (two plants/box, Figure S1) were considered as biological replicates. Before the beginning of the experiment, four groups of 24 boxes were randomly chosen to be analyzed (and destroyed) at each sampling time.

Growth conditions

Seeds were surface sterilized by immersion in NaClO 2.5% for 15 min and subsequently in a solution of Plant Preservative Mixture 50% (PPM™ Plant Cell Technology, Washington DC) for 10 min. Seeds were then germinated in sterile Petri dishes containing water for 96 h at 22 °C in the dark. Plantlets were transplanted in sterile plastic boxes containing 22 g of dry perlite. The following nutrient solutions were used to set up the different P treatments: a) Pi treatment: $Ca(NO_3)\cdot 4H_2O$ 3.5 mM; KNO_3 3.5 mM; KCl 0.6 mM; K_2SO_4 0.6 mM; $MgSO_4$ 1 mM; $NH_4H_2PO_4$ 2 mM; $MnSO_4$ 2 µM; H_3BO_3 2 µM; $CuSO_4$ 0.3 µM; $(NH_4)_6Mo7O_{24}\cdot 4H_2O$ 0.05 µM; $ZnSO_4$ 0.5 µM and Fe-EDTA 200 µM; b) Po treatment, in which $NH_4H_2PO_4$ 2 mM was replaced with NH_4NO_3 1 mM and 308 µl/l of phytic acid ($C_6H_{18}O_{24}P_6$) 50% w/w solution (Sigma-Aldrich catalogue n° 593648); c) noP treatment, in which $NH_4H_2PO_4$ 2 mM was replaced with NH_4NO_3 1 mM. The pH of the solutions was adjusted to 6.0 before use. The boxes were irrigated with 100 ml solution at transplanting and with 70 ml, 70 ml, 100 ml, 100 ml, 200 ml, 200 ml, and 200 ml of fresh nutrient solution at 6, 10, 13, 17, 20, 24 and 27 days after transplanting (DAT), respectively; the remaining solution was discarded before introducing the fresh one. Growth chamber parameters: 16 h light at 22 °C and 8 h dark at 20 °C.

Determination of maize biomass and P concentration

At 7, 14, 21 and 28 DAT the maize plants were harvested. Eight boxes for each combination population x P treatment x sampling time, were oven dried at 50°C for 48 h and shoot and root dry weight were determined.

The shoot and root of four boxes for each combination population x P treatment x sampling time were analyzed for P concentration: 0.5 g of dried tissues were reduced to ash in the muffle (550 °C for 8 h), the ashes were dissolved in 10 ml of HCl 2N and the volume was brought to 100 ml with deionized water. P concentration was determined by colorimetric (molybdenum-blue reaction) assay [30]. P use efficiency (PUE) was calculated as $(U_P - U_0)/ F_P$, where $U_P - U_0$ are the P taken up by plants with (U_P) and without (U_0) added P and F_P is the amount of P applied [31].

Root samples were screened for the presence of arbuscular mycorrhizal fungi (AMF). The analysis was performed on total RNA from 24 bulk samples (bulk of four boxes for every population x P treatment x sampling time combination) as described in Lumini et al. [32] using AMV4.5NF and AMDGR primers (Table S1).

Maize root phytase activities

Four biological replicates for each combination population x P treatment x sampling time were used for every enzymatic determination. The phytase activity in intact root (root-associated activity) and in the external solution (root-released activity) was determined as described by Richardson et al., [33], using 8 ml, 12 ml, 16 ml, and 24 ml of MES/Ca buffer solution for the incubation of the bulk samples at 7, 14, 21 and 28 DAT, respectively. Phytase activity was calculated from the release of Pi using the colorimetric molybdenum-blue reaction assay [30].

Maize root RNA-seq analysis

Maize roots were sampled at 7, 14, 21 and 28 DAT, frozen in liquid nitrogen and stored at −80 °C. From root samples of experiments B and D for P1547 hybrid and VA572, respectively, ten samples at different P treatment x sampling time combinations were selected, resulting in twenty total samples for RNA-seq analysis (Table S2). Total RNA was extracted from bulk samples (two plants of the same box) using Spectrum plant total RNA kit with DNase (Sigma-Aldrich).

The library preparation, sequencing and differential expression analysis were performed by IGA Technology service (www.igatechnology.com). RNA samples were quantified and quality tested by Agilent 2100 Bioanalyzer RNA assay (Agilent technologies, Santa Clara, CA). Final libraries were checked with both Qubit 2.0 Fluorometer (Invitrogen, Carlsbad, CA) and Agilent Bioanalyzer DNA assay. Base calling, demultiplexing and adapter masking were performed using Illumina BCL Convert v3.9.3. Reads were then processed for removing lower quality bases and adapters by ERNE software [34] and aligned on reference Zeamays.AGPv4 genome (www.maizegdb.org; [35]) with STAR [36]. RSeqQC package [37] was used to perform Statistics on "strandness" of reads, genebody coverage and read distribution.

DESeq2 package [38, 39] was used to calculate the gene-normalized expression values and to identify

differentially expressed genes (DEGs) in the different pairwise comparisons. Normalization was performed using the median-of-ratios method; statistical significance was determined using a Wald test [38]. Genes showing an FDR-adjusted *P*-value (P_{adj}) < 0.05 in the pairwise comparisons were considered as DEGs.

The Gene Ontology enrichment analysis [40] was performed by GENE ONTOLOGY (http://geneontology.org/, [41, 42]) on RNA-seq DEGs identified in P treatments within population comparisons (HPo vs HPi and VPo vs VPi); the FDR value of 0.01 was the threshold for significantly enriched GO.

Real-time qPCR

Root RNA was extracted as described above from four boxes of Pi and Po treatment for each population x sampling time combination of trial B (P1547 hybrid) and D (VA572); in total, 32 samples for each maize population were analysed. cDNA was obtained by iScript cDNA Synthesis Kit (Bio-Rad) starting from 1 µg of RNA; 0,6 µg of cDNA were used as template in a 10 µl reaction containing SSoFast EvaGreen supermix (BioRad) and specific primers for selected genes (Table S1). All PCR reactions were carried out in three replicates each using manufacturer optimized conditions, in a RotorGene 6000 (Corbett). Data analysis was performed with Rotor-Gene 6000 series Software 1.7 (Corbett). Ct values of selected genes were normalized against the Ct values of the actin reference gene to calculate for each sample the ΔCt. Expression levels of the selected genes were calculated by the comparative Ct method using the equation $E = 2^{-\Delta\Delta Ct}$, ΔΔCt being the differences in ΔCt between Po and the corresponding Pi for every time.

Statistical analyses

Analyses of variance on maize biomass, P content/concentration/PUE and enzymatic activities were performed using the General Linear Model procedure (GLM) of SAS Software version 8c (SAS Institute Inc.) in a 2×2 factorial design with P treatments and sampling time as factors and experiments as temporal repetitions. Linear contrasts were used for comparison of specific means. The CORR procedure of SAS was used for the correlation between Real-time qPCR and RNA-seq expression data of the 13 chosen DEGs.

In the case of Real-time qPCR analysis, the comparative Ct method generated expression values > 1 and < 1, whose variances were proportional to the squares of the means; consequently, a logarithmic transformation (log_2) was applied to the expression values to equalize the variances.

Results

Maize biomass and P concentration

P treatment, as main source of variation, showed a highly significant effect on root and shoot growth in both the maize populations (Fig. 1b and Table S3). The absence of P (noP treatment) did not significantly affect plant growth until 14 DAT while from this time on a significant difference in shoot biomass in noP compared to Pi and Po treatments was observed in both populations (Fig. 1b) and symptoms of P starvation, e. g. accumulation of anthocyanins [43], became evident in leaves (Fig. 1a). At 21 DAT, Pi and Po treatments had a similar effect on root and shoot growth of VA572 population while in P1547 hybrid Pi treatment showed greater root and shoot growth than Po. At 28 DAT, inorganic Pi treatment supported in both populations a significantly greater root and shoot biomass compared to Po treatment (Fig. 1b), in which leaves were generally characterized by the presence of yellow stripes (Fig. 1c).

Different from biomass, P concentration of plant tissues was earlier affected by the absence of P as since 7 DAT the noP treatment significantly reduced root and shoot P concentration in both the maize populations (Fig. 1d). No significant differences in P concentration were in general observed between Po and Pi treatments; however, at 21 and 28 DAT, Po treatment in VA572 roots determined significantly greater values (Fig. 1d). The calculated P content parameter (P concentration x DM) and PUE confirmed at 28 DAT a similar effect of Pi and Po treatments in roots and a prevailing effect of Pi over Po treatment in shoots for both populations (Figure S2a and b).

No colonisation by AMF was detected in any root sample of both the maize populations (Figure S3) thus indicating that the use of $InsP_6$ as P source can be ascribed solely to plant strategies.

Taken together, these results indicated that the two maize populations were able to grow, over the time of 28 DAT considered in this study, using phytic acid as the sole P source, although this source resulted less efficient than inorganic phosphate at 28 DAT in terms of root and shoot biomass and shoot P content.

Enzymatic activity

The root-released phytase activity was considered the most indicative of the root secreted phytase activities. Despite a wide variation of activity values, in both maize populations a significant root-released phytase activity was mainly detected in Po treatment (Fig. 2). In P1547 hybrid, two peaks of phytase activity were found at 7 and 21 DAT, while in VA572 population the phytase activity was present since 14 DAT and strongly increased at 28 DAT in Po and noP treatments (Fig. 2).

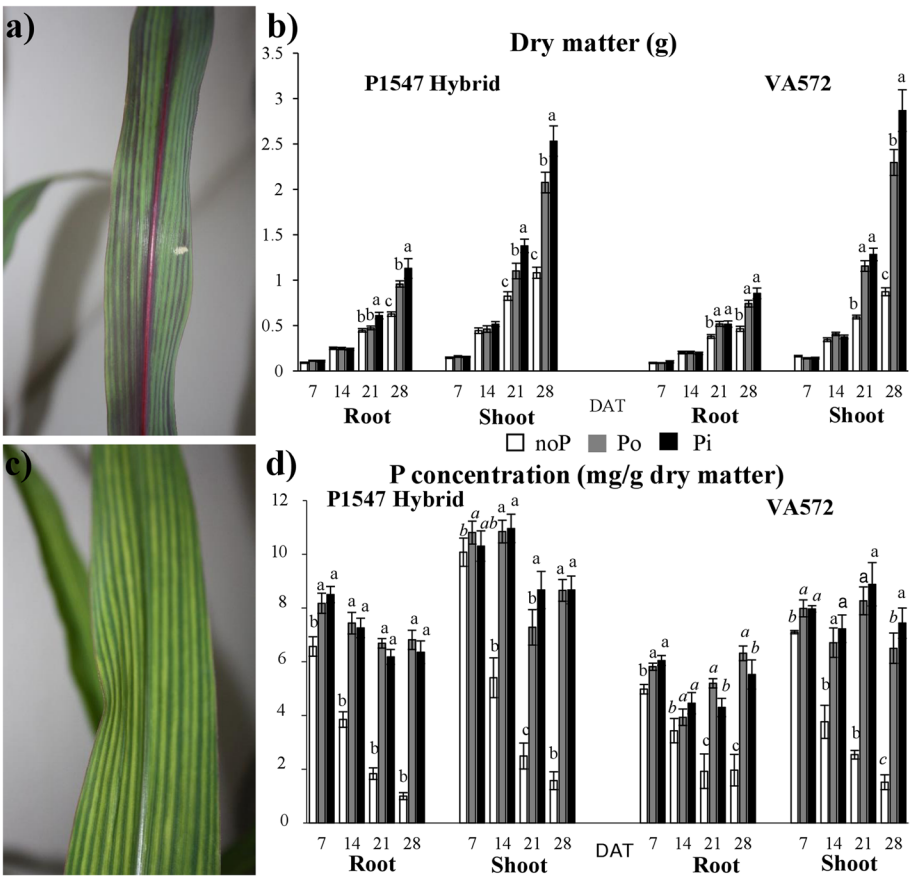

Fig. 1 Plant bio-agronomic parameters. **a** P deficiency symptoms in leaves of noP treatment plants. **b** Root and shoot DM of the different population x P treatment x sampling time combinations (means of the two trials per population). **c** Yellow stripe symptoms in leaves of Po treatment at 28 DAT. **d** Root and shoot P content (mg/g dry matter) of the different population x P treatment x sampling time combinations (means of the two trials per population). Values are means ± SE; different letters above bars indicate significant differences ($p < 0.05$, italic; $p < 0.005$, normal font) among treatments within sampling times by linear contrasts. Only significant differences are indicated

No significant differences among treatments and sampling times were found for the root- associated phytase activity in P1547 hybrid, because of a wide among-replicate variation; in VA572 population, a significantly greater activity in noP treatment was present at 28 DAT (Table S3 and Figure S4).

These results indicated that a root-released phytase activity was present in maize roots and suggested it was induced by the presence of $InsP_6$ as P source.

RNA-seq analysis

To investigate the strategies displayed by the two maize populations in the use of phytic P compared to inorganic phosphate, an RNA-Seq analysis was run on twenty root samples obtained from Po and Pi treatments of P1547 hybrid (H) and VA572 (V) populations. The analysis generated a mean of 37,96 million high-quality reads per sample, 72.66% of which mapped to the maize B73 reference genome with 62.4% of these representing uniquely mapped reads (Table S2). The alignment on the reference Zeamays.AGPv4 genome resulted in 32,079 genes (Data S1). The differentially expressed genes (DEGs) specific to populations H and V, P treatments and sampling times were identified by comparing the populations within P treatment (HPo vs VPo and HPi vs VPi, Table S4), P treatments within population (HPo *vs* HPi and VPo *vs* VPi, Table S5) and P treatments within time (14DATPo *vs* 14DATPi, 21DATPo *vs* 21DATPi, 28DATPo *vs* 28DATPi, Table S6).

A PCA analysis based on the whole dataset of 32,079 genes per root sample after variance stabilizing transformation (Data S1) clearly differentiated the two maize populations along the PC1 component. Pi and Po treatments were distinguished along the PC2 component in VA572 population, while a clear distinction was not evident in P1547 hybrid (Fig. 3a). No clear differences were put in evidence among different sampling times (7, 14, 21 and 28 DAT) in neither the populations (Fig. 3a). A

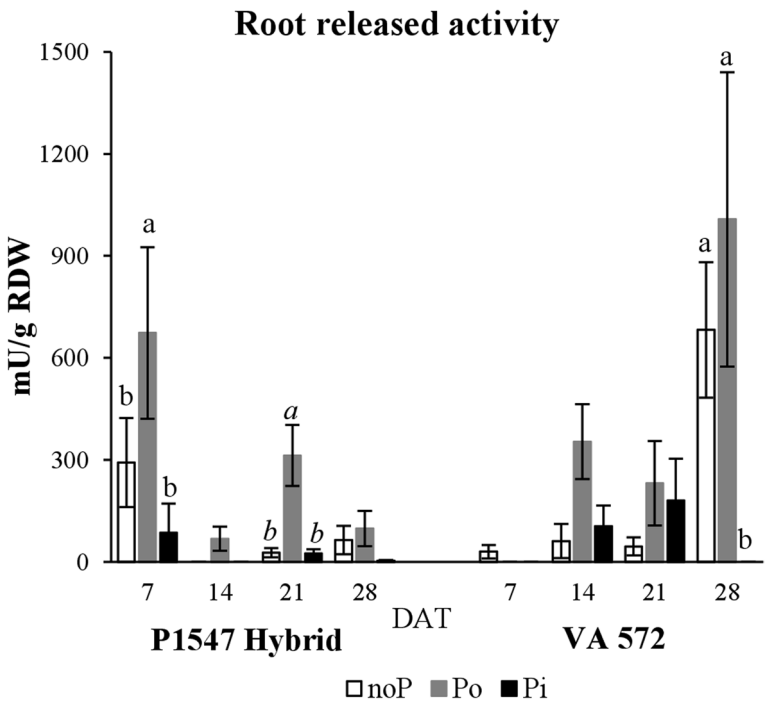

Fig. 2 Root-released phytase activity of the different population x P treatment x sampling time combinations. Values are means ± SE of the two trials per population; different letters above bars indicate significant differences ($p < 0.05$, italic; $p < 0.005$, normal font) among treatments within sampling times by linear contrasts. Only significant differences are indicated

larger internal variation in VA572 population compared to P1547 hybrid was also evident from PCA plot (Fig. 3a) and confirmed by the clustering of the same data (Figure S5).

The number of DEGs differentiating the two populations was the same in the two P treatments: 4112 in Pi and 4111 in Po; 1739 DEGs, 42.30% of the total, were present in both the P treatments (common DEGs, Fig. 3b) and was similarly distributed in up and down regulated genes in the two treatments (Fig. 3c). The DEGs specific to each P treatment (non-common DEGs), 2373 and 2372 respectively for Pi and Po, were evenly distributed in up and down regulated in Pi treatment while in Po treatment the majority was downregulated (1558/2372, i.e. 66%) with respect to the upregulated DEGs (814/2372, i.e. 34%) (Fig. 3c). Then, about two third of the DEGs specific to Po treatment had a lower expression in P1547 hybrid compared to VA572 population.

The expression pattern of Po *vs* Pi treatment varied greatly in the two populations for the number of DEGs involved: 58 in the case of P1547 hybrid and 618 in the case of VA572 population. Six DEGs were present in both populations (common DEGs, Fig. 3b) and were all downregulated (Fig. 3d). The DEGs specific to each population (non-common DEGs), 52 and 612 for P1547 hybrid and VA572 respectively, were mainly downregulated in the hybrid (45/52, i.e. 86.54%) while mainly upregulated in VA572 population (503/612, i.e. 82.19%) (Fig. 3d).

Taken together, these data indicated that the expression pattern in the comparison Po *vs* Pi treatment was characterized by the overexpression of a large number of genes in the case of VA572 and by the repression of a reduced number of genes in the case of P1547 hybrid.

Phytase/phosphatase genes

To identify possible candidate genes responsible for the root-released phytase activity found in both maize populations (Fig. 2), the presence among DEGs of the two phytase genes Zm00001d041660 and Zm00001d041670, involved in the mobilization of phytin globoids in radicle cortex during early germination phases [44], was examined without success. Acid phosphatases (AP) and in particular the purple AP (PAP) family represent a major route for plant cleavage of phosphate from organic P sources: eight PAPs differentiated the two populations in Po (Zm00001d053099, Zm00001d043291, Zm00001d023404), in Pi (Zm00001d025343, Zm00001d034839) and in both treatments (Zm00001d003990, Zm00001d033566, Zm00001d023410) (Table 1, Table S4). On the contrary, a single candidate PAP-encoding gene, Zm00001d027731, was among the Po *vs* Pi DEGs in VA572 (Table 1,

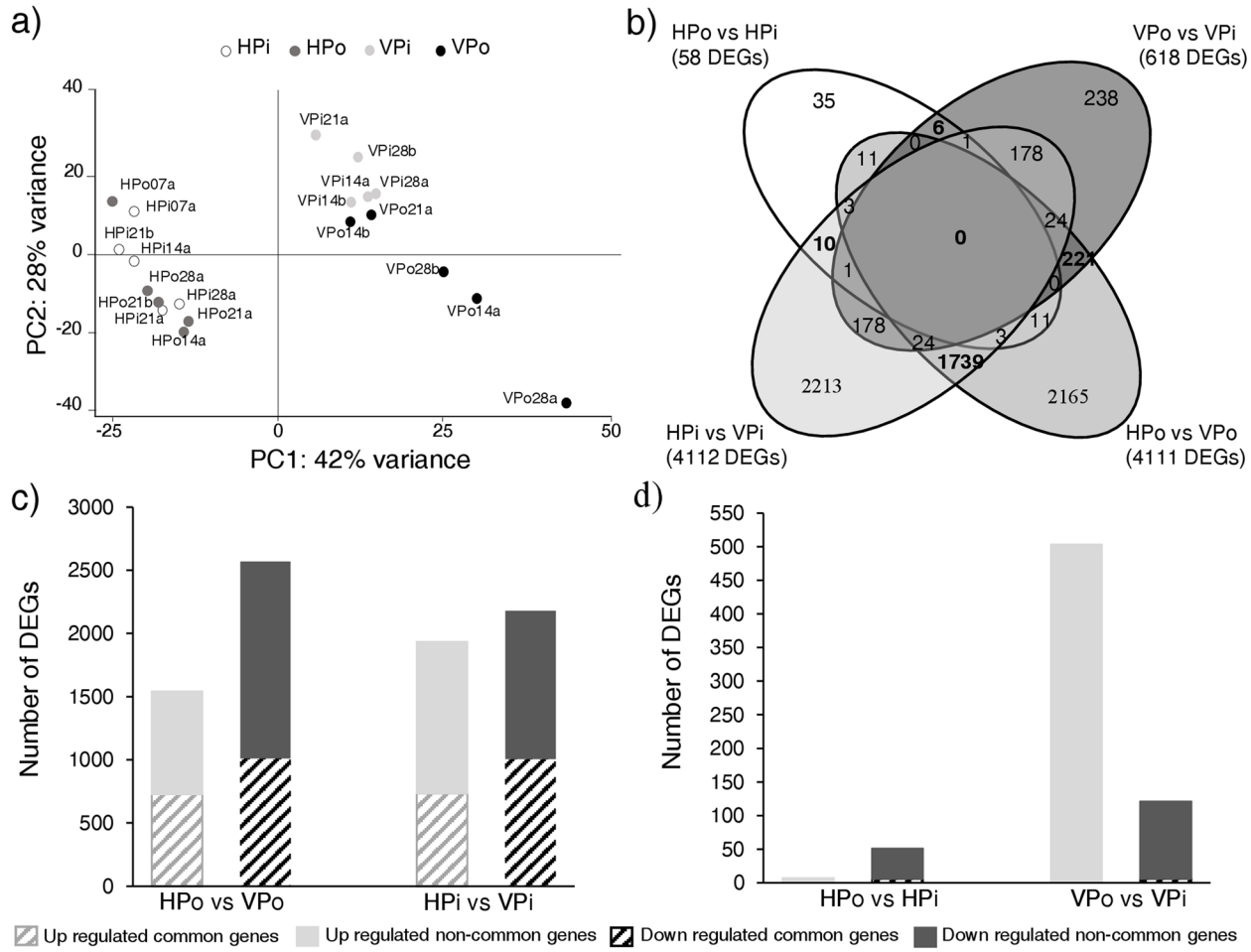

Fig. 3 RNA-seq analysis on the twenty selected root samples. **a** Principal Component Analysis on the whole dataset of 32,079 genes per root sample of P1547 Hybrid (H) and VA572 (V) populations in Pi and Po treatments at 7, 14, 21, 28 DAT. **b** Venn diagram of DEGs in the four comparisons considered. Numbers in the overlapping areas represent common genes; numbers in non-overlapping areas represent DEGs specific to the corresponding comparison. **c** and **d** Number of up and down regulated DEGs, split in common and non-common, in the different comparisons analysed

Table S5). This gene, however, was not retained among candidate maize PAP because of the absence of three PAP conserved residues out of five [29]. Zm00001d027731 was also significantly upregulated in the comparison HPi *vs* VPi, i.e. more expressed in P1547 hybrid than in VA572 population in Pi treatment, thus making it one of the 100 more expressed genes in our whole dataset (Table 1).

Phosphate signaling pathway

Zm00001d042935, considered an early responsive gene to LP stress in maize [45], was among the upregulated DEGs only when comparing 14DAT Po *vs* 14DAT Pi (Table 1, Table S6), possibly corresponding to the seedling transition from the prevailing use of seed P reserves to the Po uptake from the medium.

Phosphate starvation response (*ZmPHR*) genes, members of the MYB transcription factors (TF), are known to regulate phosphate homeostasis in plants; among the 18 *ZmPHR* genes identified in the maize genome [46], a common DEG (Zm00001d015226) downregulated in both the comparisons HPi *vs* VPi and HPo *vs* VPo and a DEG (Zm00001d038546) upregulated in HPi *vs* VPi distinguished the two populations (Table 1, Table S4). Instead, in VA572 population a single DEG (Zm00001d020019), coding for the PHR1-LIKE 3 protein, was downregulated in Po *vs* Pi treatment (Table 1, Table S5). As PHR induction of phosphate starvation-induced (PSI) genes can be inhibited by the association with SPX proteins [47, 48], the presence of *SPX* genes among DEGs was also examined. Zm00001d044541 was one of the seven upregulated DEGs in P1547 hybrid (HPo *vs* HPi comparison Fig. 3d, Table 1, Table S5); the

Table 1 Log_2 fold change values of DEGs discussed in the text in the different comparisons. Genes selected for Real-time qPCR analysis are indicated in bold

Gene ID	Gene description	HPo vs HPi	VPo vs VPi	HPi vs VPi	HPo vs VPo	14DAT Po vs Pi	28DAT Po vs Pi
Phytase/Phosphatase activity							
Zm00001d053099 (Zm00001eb201680)	Purple Acid Phosphatase (*ZmPAP*)				4.14		
Zm00001d043291 (Zm00001eb151650)	Purple Acid Phosphatase (*ZmPAP*)				1.19		
Zm00001d023404 (Zm00001eb406620)	Purple Acid Phosphatase (*ZmPAP*)				−1.54		
Zm00001d025343 (Zm00001eb421880)	Purple Acid Phosphatase (*ZmPAP*)			−1.35			
Zm00001d034839 (Zm00001eb064450)	Purple Acid Phosphatase (*ZmPAP*)			1.63			
Zm00001d033566 (Zm00001eb053560)	Purple Acid Phosphatase (*ZmPAP*)			6.16	3.21		
Zm00001d003990 (Zm00001eb085600)	Purple Acid Phosphatase (*ZmPAP*)			6.54	4.67		
Zm00001d023410 (Zm00001eb406650)	Purple Acid Phosphatase (*ZmPAP*)			−2.61	−3.77		
Zm00001d027731[a] (Zm00001eb004420)	**putative Purple Acid Phosphatase (putative PAP)**		1.60	1.05			
Phosphate signalling pathway							
Zm00001d042935 (Zm00001eb148590)	Induced Phosphate Starvation 1 (*ZmIPS1*)					1.23	
Zm00001d015226 (Zm00001eb232000)	Phosphate starvation response gene (*ZmPHR*)			−2.00	−2.61		
Zm00001d038546 (Zm00001eb291350)	Phosphate starvation response gene (*ZmPHR*)			1.06			
Zm00001d020019 (Zm00001eb309360)	Phosphate starvation response gene (*ZmPHR1-like 3*)		−1.42				
Zm00001d044541 (Zm00001eb162710)	**SPX domain-containing protein4 (*ZmSPX4*)**	1.93					
Zm00001d051945 (Zm00001eb191650)	SPX domain containing phosphate transporter 2			1.53			
Zm00001d029460 (Zm00001eb019570)	SPX domain containing protein 7				3.45		
Zm00001d038972 (Zm00001eb295490)	ubiquitin-conjugating E2 enzyme (*ZmPHO2*)				−0.73		
Zm00001d032850 (Zm00001eb047070)	PHT1 gene family (*ZmPHT1;9*)			1.27			
Zm00001d027700 (Zm00001eb004100)	PHT1 gene family (*ZmPHT1;13*)			−5.95			
Maize inositol phosphate metabolism							
Zm00001d044442 (Zm00001eb161780)	**ABC transporter G family member 40**		3.38		−3.77	3.89	
Zm00001d046234 (Zm00001eb384280)	Inositol oxygenase 2		−1.15	−1.54			
Zm00001d027625 (Zm00001eb003490)	**ABC transporter (*ZmMRP4*)**		0.94		−0.74		
Zm00001d053333 (Zm00001eb203680)	**Sec14-like phosphatidylinositol transfer protein**		5.85	5.68			
Zm00001d038530 (Zm00001eb291170)	**Putative inositol polyphosphate phosphatase (*ZmPROH9*)**		1.66	1.65			
Zm00001d041608 (Zm00001eb137020)	Inositol-phosphotransferase 1		2.52		−2.00		

Table 1 (continued)

Gene ID	Gene description	HPo vs HPi	VPo vs VPi	HPi vs VPi	HPo vs VPo	14DAT Po vs Pi	28DAT Po vs Pi
Zm00001d037160 (Zm00001eb279030)	**Nodulin-like protein**		5.74		−2.43		
Zm00001d022636 (Zm00001eb332090)	**Major Facilitator Superfamily protein (*ZmNPI611a*)**		2.53			1.83	
Root system development							
Zm00001d040035 (Zm00001eb125660)	Low phosphate root 1b (*ZmLPR1b*)		2.16	1.30			
Zm00001d032732 (Zm00001eb046080)	cyclin-dependent kinase inhibitor 1 (*ZmCKI1*)		1.07		−0.86		
Zm00001d003311 (Zm00001eb079790)	dioxygenase for auxin oxidation1 (*ZmDAO1*)		2.82		−2.06		
Zm00001d018414 (Zm00001eb258220)	TF aux/IAA24 (*ZmAUX/IAA24*)		3.21		−2.72		
Zm00001d039624 (Zm00001eb122410)	TF aux/IAA8 (*ZmAUX/IAA8*)		1.27				
Zm00001d038165 (Zm00001eb287800)	GID1-like gibberellin receptor (*ZmGID1*)		2.03			1.84	
Zm00001d039520 (Zm00001eb121500)	**Cytokinin oxidase 1 (*ZmCKO1*)**		4.94	2.41			
Zm00001d036416 (Zm00001eb272410)	**Calcium dependent protein kinase13 (*ZmCDPK13)***		2.06		−2.01		
Zm00001d049020 (Zm00001eb168290)	**Root preferential 1 (*ZmRTP1*)**		−2.44				
Zm00001d043019 (Zm00001eb149240)	Laccase 9 (*ZmLAC9*)	−1.85	−2.19				
Zm00001d010308 (Zm00001eb349710)	GID1-like gibberellin receptor (*ZmGID2*)			0.64			
Zm00001d030993 (Zm00001eb031190)	TF aux/IAA2 (ZmAUX/IAA2)				1.32		
Zm00001d052112 (Zm00001eb193180)	Growth regulatory factor (*ZmGRFTF10*)	1.03			1.39		
Uptake, transport and assimilation of macro and micronutrients							
Zm00001d054057 (Zm00001eb209670)	**Nitrate transport 2 (*ZmNRT2.1*)**	−3.28					
Zm00001d054060 (Zm00001eb209690)	Nitrate transport 1 (*ZmNRT2.2*)	−4.37			−3.58		
Zm00001d006823 (Zm00001eb108840)	Nitrate transporter (*ZmNPF8.18*)		−1.49				
Zm00001d031769 (Zm00001eb037860)	Nitrate reductase (*ZmNNR4*)		3.24		−2.24		
Zm00001d049995 (Zm00001eb176470)	Nitrate reductase (*ZmNNR1*)		1.56	1.68			
Zm00001d003859 (Zm00001eb084600)	High-affinity K^+ transporter (*ZmHAK20*)		−6.73		7.39		
Zm00001d037289 (Zm00001eb280210)	Outward rectifying potassium channel1 (*ZmORK1*)		1.84		−1.66		
Zm00001d003555 (Zm00001eb081780)	Potassium channel SKOR		2.60	1.51	−2.10	2.60	
Zm00001d029360	Starch synthase 1b		−5.50	−7.41			−5.80
Zm00001d045042[a] (Zm00001eb374090)	**Sucrose synthase 1 (*ZmSH1*)**		2.47			2.01	
Zm00001d017121[a] (Zm00001eb246370)	glyceraldehyde-3-phosphate-dehydrogenase (*ZmGPC4*)		1.37				
Zm00001d045431[a] (Zm00001eb377870)	Enolase (*ZmENO1*)		1.62		−1.73		

Table 1 (continued)

Gene ID	Gene description	HPo vs HPi	VPo vs VPi	HPi vs VPi	HPo vs VPo	14DAT Po vs Pi	28DAT Po vs Pi
Zm00001d018429 (Zm00001eb258360)	Phosphoenolpyruvate carboxylase kinase (*ZmPPCK19*)		3.64			3.54	
Zm00001d033931[a] (Zm00001eb056510)	Alcohol dehydrogenase (*ZmADH1*)		2.31			1.12	
Zm00001d049059[a] (Zm00001eb168550)	Alcohol dehydrogenase (*ZmADH2*)		2.08		−1.42		
Zm00001d017429 (Zm00001eb249020)	yellow stripe 1 transporter of Fe-phytosiderophores (*ZmYS1*)	1.36					2.85
Zm00001d042062 (Zm00001eb140680)	bHLH transcription factor (*ZmbHLH126*)	2.31					3.29
Zm00001d041352 (Zm00001eb135050)	Adenine phosphoribosyltransferase2 (*ZmAPT*)	0.53					
Zm00001d041111 (Zm00001eb133440)	yellow stripe 3 transporter of Fe-phytosiderophores (*ZmYS3*)		3.43				4.37
Zm00001d052435 (Zm00001eb196180)	Transporter of the phytosiderophores mugineic acids (*ZmTOM2*)		5.35		−3.59		5.23

[a] DEGs included in the 100 most expressed genes

variant *ZmSPX4.2* of this gene was proved to interact with *ZmPHR1* by yeast two-hybrid assay [48]. Other two *SPX* genes—Zm00001d029460, implied in phosphate starvation response, and Zm00001d051945, phosphate transporter 2—were among the DEGs upregulated in HPo *vs* VPo and HPi *vs* VPi comparisons, respectively (Table 1, Table S4).

Consistent with the negative regulation of *PHR* genes in Po treatment, the P transporters belonging to the *PHT1* gene family [49] and targeted by the PHR-SPX complex [50], were absent among the DEGs differentiating the two populations in Po treatment and present only in Pi: Zm00001d032850, more expressed in P1547 hybrid, and Zm00001d027700, more expressed in VA572 population (Table 1, Table S4).

Maize inositol phosphate metabolism

Among the genes implied in co-expression networks related to inositol phosphate metabolism in maize [51], only the ABC transporter Zm00001d044442, upregulated in VPo *vs* VPi comparison and Zm00001d046234, involved in inositol catabolic process and downregulated in the same comparison, differentiated the two P treatments in VA572 population (Table 1, Tables S5). Other transmembrane transporters, upregulated in VPo *vs* VPi comparison, were represented by the ABC transporter gene Zm00001d027625, known for its effect on seed phytate content in maize [52], the nodulin-like family gene Zm00001d037160 and the major facilitator superfamily gene Zm00001d022636 (Table 1, Table S5). Both the *Arabidopsis* orthologs At4g34950 and At2g16660 of Zm00001d022636 were found being involved in root regulators of phosphate starvation response networks [53].

These findings suggested that in Po treatment highly phosphorylated inositol phosphates could be the object of a direct root uptake and further directed by internal transfer to metabolic pathways based on these compounds.

The synthesis of phosphoinositides (PIPs) represented the inositol phosphate-based pathways largely involved in our dataset. In fact, the genes Zm00001d053333, coding for a Sec14-like phosphatidylinositol transfer protein regulating the homeostasis of PIPs [54], Zm00001d038530, involved in phosphatidylinositol dephosphorylation, and Zm00001d041608, a phosphotransferase synthetizing the SL inositol phosphoryl ceramide, were all upregulated in VPo *vs* VPi comparison (Table 1, Table S5).

The genes Zm00001d037160, Zm00001d044442, Zm00001d027625 and Zm00001d041608 turned out to be also more expressed by VA572 in HPo *vs* VPo comparison while Zm00001d046234 in HPi *vs* VPi comparison; on the contrary, Zm00001d053333 and Zm00001d038530 were more expressed in P1547 hybrid in HPi *vs* VPi comparison (Table 1, Table S4).

Root system development

The upregulation of the genes Zm00001d040035, a negative regulator of primary root elongation in LP condition [55], and the cyclin-dependent kinase inhibitor Zm00001d032732, a negative regulator of cell division and growth, suggested a reduction of primary root

growth and an inhibition of lateral root development in VPo *vs* VPi comparison (Table 1, Table S5).

Auxin and gibberellic acid (GA) signaling are known to play important roles in this process [55, 56] and in fact the auxin-related genes Zm00001d003311, the transcriptional repressors Zm00001d018414 and Zm00001d039624 and the gibberellin receptor Zm00001d038165, were also found among the upregulated DEGs in VPo *vs* VPi comparison (Table 1, Table S5). The cytokinin oxidase Zm00001d039520 was among the upregulated DEGs in VPo *vs* VPi comparison as well as the calcium-dependent protein kinase Zm00001d036416, identified as a candidate gene in a GWAS study for Root System Architecture traits in maize [57] and more expressed in VA572 in HPo *vs* VPo comparison (Table 1, Tables S4 and S5).

Modifications of cell wall structure appeared to occur in VA572 as suggested by the down regulation of the gene Zm00001d049020, involved in suberin pathway [5], and Zm00001d043019, participating in lignin polymer formation (Table 1, Table S5); this last gene was also downregulated in HPo *vs* HPi comparison (Table 1, Table S5).

Taken together these results suggested that VA572 population was subjected to root morphology changes induced by Po treatment and dependent on the modification of gene expression mediated by auxin, GA and cytokinin signaling.

In P1547 hybrid, the genes Zm00001d040035, Zm00001d010308, belonging to the same gene family of Zm00001d038165, and Zm00001d039520 were present among the DEGs in HPi *vs* VPi comparison where they were expressed at higher level in the hybrid than in VA572 populations as the transcriptional repressor Zm00001d030993 in HPo *vs* VPo comparison (Table 1, Table S4). However, the only root development-related gene induced by Po treatment in P1547 hybrid was the growth regulatory TF Zm0001d052112 (Table 1, Table S5), highly expressed in maize roots [58] as its ortholog *OsGRF6* positively regulating root development in rice [59]. Thus, in P1547 hybrid Zm0001d052112 appeared a key factor in the root morphology changes induced by Po treatment mediated by auxin, GA and cytokinin signaling networks.

Relationship of P sources with N and K macronutrients and micronutrients

Both the high affinity nitrate transporters Zm00001d0054060 and Zm00001d0054057, displaying a root-specific expression profile [60, 61], were among the downregulated DEGs in HPo *vs* HPi comparison (Table 1, Table S5). In VPo *vs* VPi comparison, the low-affinity nitrate transporter Zm00001d006823 was also downregulated; instead, two nitrate reductase genes Zm00001d031769 and Zm00001d049995, acting in nitrate reduction into nitrite in cytoplasm, were among the upregulated DEGs in VPo *vs* VPi (Table 1, Table S5).

Considering K uptake, the high-affinity K^+ transporter Zm00001d003859 [62] was downregulated in VPo *vs* VPi, while the K channels Zm00001d037289 and Zm00001d003555 were upregulated, this last also being highly constitutively expressed by P1547 hybrid in Pi treatment and present in 14DATPo *vs* 14DATPi comparison (Table 1, Tables S4, S5, S6).

Sugar metabolism was largely affected by Po treatment in VA572 roots: the granule-bound starch synthase 1b gene (Zm00001d029360), involved in starch synthesis [63], was downregulated in VPo *vs* VPi (Table 1, Table S5) and in 28DATPo *vs* 28DATPi comparisons (Table 1, Table S6). On the contrary, several genes acting on primary sugar metabolism (Zm00001d045042), glycolysis (Zm00001d017121, Zm00001d045431, Zm00001d018429) and anaerobic sugar metabolism (Zm00001d033931, Zm00001d049059) were upregulated in VPo *vs* VPi (Table 1, Table S5). Zm00001d045042, Zm00001d017121, Zm00001d045431, Zm00001d033931 and Zm00001d049059 were also among the 100 most expressed genes in our dataset (Table 1).

The genes Zm00001d017429, an oligopeptide transporter of Fe(III)-phytosiderophores [64], Zm00001d042062, a bHLH TF ortholog of *OsIRO2* induced in rice shoots and roots by Fe deficiency [65] and Zm00001d041352, involved in the synthesis of the Fe chelator mugineic acid [66], were found among the upregulated DEGs in HPo *vs* HPi, Zm00001d017429 and Zm00001d042062 being also present in 28DATPo *vs* 28DATPi comparison (Table 1, Tables S5 and S6). In VPo *vs* VPi and 28DATPo *vs* 28DATPi comparisons, the Fe(III)-phytosiderophore transporters Zm00001d041111 and Zm00001d052435 resulted also among the upregulated DEGs (Table 1, Tables S5 and S6).

Gene ontology (GO) enrichment analysis

A GO enrichment analysis of the functional significance for the category biological process was performed on the 670 DEGs (58 from P15447 and 618 from VA572, six being common to populations) resulting from Po vs Pi comparison. The 622 uniquely mapped genes used in the analysis were grouped in ten significantly enriched (FDR < 0.01) GO terms indicated in Fig. 4. Response to stimulus (GO:0050896), Response to chemical (GO:0042221) and Transmembrane transport (GO: 0055085) were the GO terms showing the major number of DEGs involved. The DEGs present in Response to stimulus and Response to chemical GO terms included genes involved in Phosphate signalling pathway (Zm00001d044541), Root system development (Zm00001d018414, Zm00001d036416,

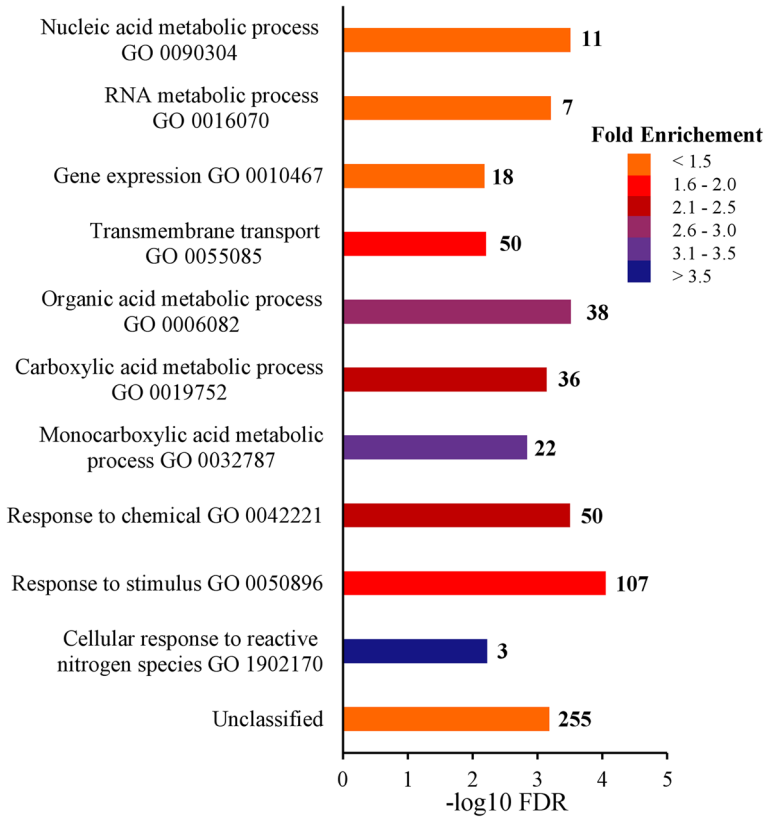

Fig. 4 GO enrichment analysis for biological processes on RNA-seq DEGs in within population P treatment comparison of both maize populations. Only GO terms with FDR values < 0.01 are considered as enriched terms. Numbers at the end of the bars represent the DEGs belonging to each GO terms

Zm00001d039624, Zm00001d040035) and Uptake of macro and micronutrients (Zm00001d054057, Zm00001d054060, Zm00001d018429, Zm00001d033931, Zm00001d049059, Zm00001d017429) reported in Table 1. Among the DEGs representing the Transmembrane transport class, Zm00001d028689, present and downregulated in both populations, was a *ZmPHR1*-regulated *PSR* gene, that is responsive to the major regulator of phosphate signaling and homeostasis, also involved in response to ABA, osmotic stress and water deprivation [67]. Two other DEGs (Zm00001d021396 and Zm00001d012938), upregulated in VPo vs VPi comparison, were annotated as phosphate ion transport in GO biological process. Besides, the root-expressed *ZmPIN9* gene (Zm00001d043179), present in Transmembrane transport and Response to chemical classes and upregulated in VPo vs VPi comparison, took part in the response to sensing heterogeneous Pi supply by modifying auxin distribution of lateral roots to increase root proliferation [68]. Other DEGs present in this GO class are involved in Maize inositol phosphate metabolism (Zm00001d044442, Zm00001d027625, Zm00001d037160) and Uptake of macro and micronutrients (Zm00001d054057, Zm00001d054060, Zm00001d006823, Zm00001d003859, Zm00001d037289, Zm00001d003555, Zm00001d017429, Zm00001d041111, Zm00001d052435) (Table 1). Among DEGs representing acid metabolic process GO terms (GO 0006082, GO 0019752 and GO 0032787, Fig. 4), genes involved in Maize inositol phosphate metabolism (Zm00001d046234) and Uptake, transport and assimilation of macro and micronutrients (Zm00001d031769, Zm00001d049995, Zm00001d017121 and Zm00001d045431) were present (Table 1). Finally, the Zm00001d052112 involved in Root system development (Table 1) was found among the DEGs representing GO 0090304, GO 0016070 and GO 0010467 (Fig. 4).

Quantitative real-time PCR analysis

A total of thirteen genes, identified as DEGs in Po *vs* Pi treatment in at least one of the two populations, were selected for quantitative real-time PCR (qRT-PCR) analysis (Table 1, in bold). The complete set of root samples along the four sampling times (7, 14, 21 and 28 DAT) was analyzed from B (P1547 hybrid) and D (VA572) experiments used for RNA-seq analysis. Considering both populations, 10 out of 13 genes showed a significant main

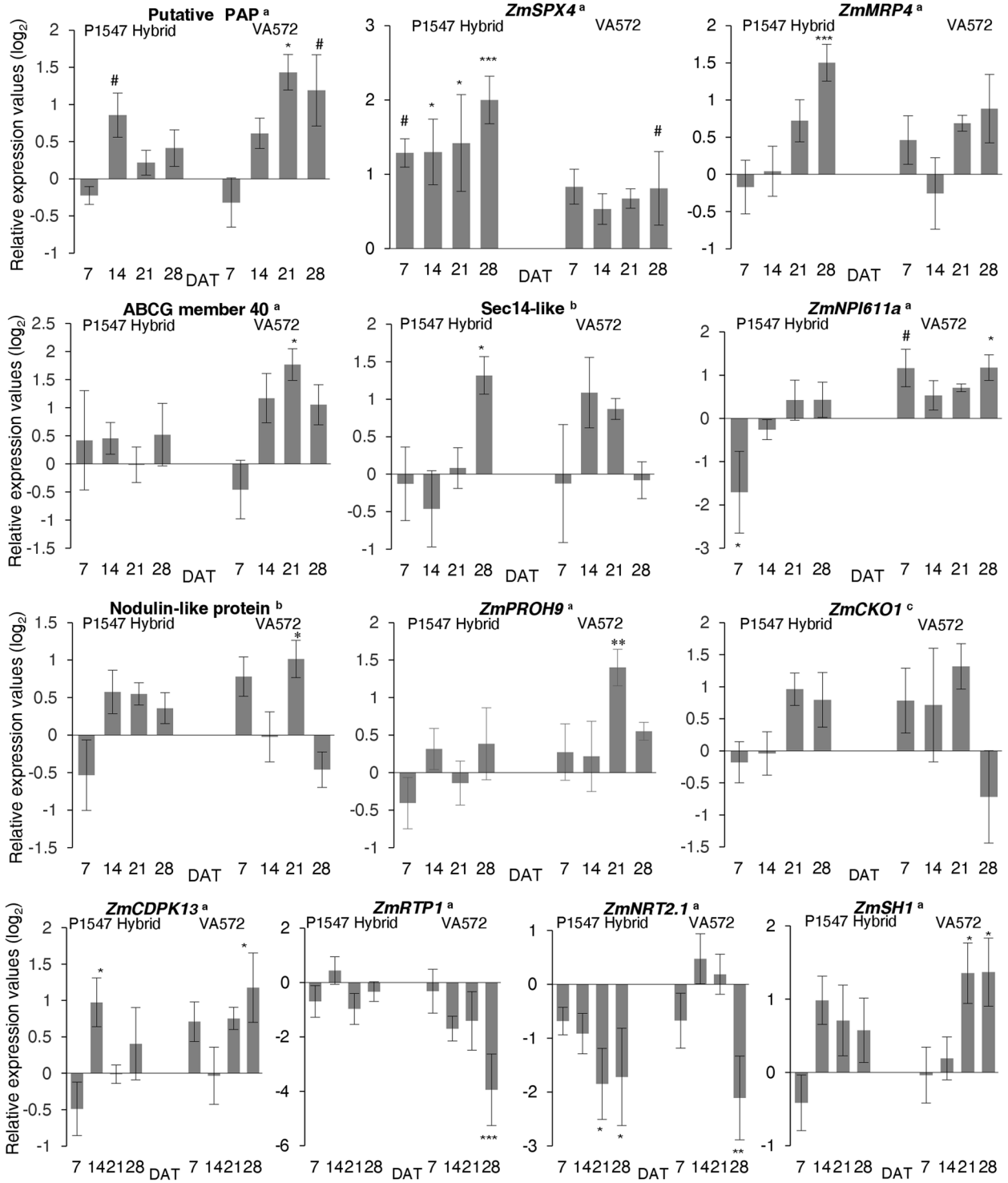

Fig. 5 Quantitative real-time PCR on the thirteen selected DEGs. Values (log_2 transformation) are the means ± SE of four biological replicates; mean significant differences by linear contrasts are indicated as $^{\#}0.05 < p < 0.08$; $^{*}p < 0.05$; $^{**}p < 0.01$; $^{***}p < 0.001$ (ANOVA). **a** significant main effect of P treatment in at least one population; **b** no significant main effect of P treatment but significant linear contrasts; **c** no significant effect of P treatment

effect of P treatment on the expression level across sampling times in the same direction found in RNA-seq analysis; in two further genes, the transporters Sec14p-like and noduline-like, the effect of P treatment was significant only for a specific sampling time and consistent with the results of RNA-seq; finally, *ZmCKO1* did not show any significant P treatment effect in both the populations, despite the increasing expression level at 21 and 28DAT in VA572 (Fig. 5).

Then, qRT-PCR results generally confirmed the expression patterns obtained by RNA-seq analysis as indicated by the significant correlation ($r = 0.73$, $p < 0.005$) found between the two sets of expression values (Figure S6). The major differences between qRT-PCR and RNA-seq concerned the significant P1547 hybrid induction at 28DAT for the transporters *ZmMRP4* and *ZmSec14-like* and the significant downregulation of *ZmNRT2.1* at 28DAT in VA572 (Fig. 5). The expression variation of these genes was relative to the only 28DAT time and then probably not able to significantly modify the gene expression level across all sampling times of the RNA-seq analysis.

For both the populations, the significant P treatment differences were present at 21 and/or at 28DAT suggesting a trend of induction along sampling times and the persistence of the induced expression patterns also longer the 28DAT term of the present study. Finally, the expression patterns of genes characterizing each population in RNA-seq analysis were maintained in qRT-PCR: *ZmSPX4* and *ZmNRT2.1*, with opposite regulation, specific to P1547 hybrid; the upregulated transporters Zm*ABCG40, ZmNPI611a*, and the sucrose synthase *ZmSH1* particular to VA572 population together with the downregulated root development-related *ZmRTP1*.

It is interesting to note that the putative PAP Zm00001d027731, induced in VA572 population at 21 and 28DAT in both RNA-seq and qRT-PCR analysis, resulted induced also in P1547 hybrid in qRT-PCR ($0.08 < p > 0.05$ at 14DAT, Fig. 5); as seen before in the case of *ZmSPX4* and *ZmNRT2.1* genes, such an expression pattern suggests that the differences between the two populations in the responses to Po treatment could be in some case less clear cut than indicated in RNA-seq analysis and that some genes could play a transient role in both the populations at specific times.

Discussion

Both maize populations were able to use phytic acid for growth during a 28DAT span

In both maize populations the Po treatment sustained a significantly greater tissue P content and biomass growth with respect to noP treatment since 7 and 14DAT, respectively (Fig. 1) indicating a phosphate hydrolysis in the medium by AMF-free plant roots. The significantly higher level of root-released phytase/phosphatase activity in Po treatment suggested an induction by the presence of $InsP_6$. An enhancement of root phosphatase release in *Trifolium alexandrinum* grown in aseptic culture with phytin as P source was also observed by Tarafdar and Claassen [69]. However, $InsP_6$ source in our experiment was utilized less efficiently than Pi in both the populations, except for VA572 root at 21 DAT. The 2 mM rate of P from $InsP_6$, equivalent to that from Pi source, was not limiting in our experimental conditions as a tenfold rate of 20 mM $InsP_6$ did not affect maize growth and P uptake at 28 DAT (data not presented), excluding also significant $InsP_6$ sorption by perlite substrate and/or precipitation by reaction with mineral cations. Thus, $InsP_6$ availability for plant growth did not appear a limiting step in P acquisition in our experimental conditions as, on the contrary, found by other authors working with agar or sand-vermiculite media [70, 71]. Findenegg and Nelemans [72] comparing maize growth and P uptake with 2 mM Ca-phytate *vs* Pi sources also found a better efficiency of Pi and an improved P uptake from phytate source with addition of a phytase of microbial origin, thus concluding that the rate of phytin hydrolysis was a limiting step in the use of phytate. The presence of the PAP-encoding gene Zm00001d027731 among the 100 more expressed genes in our whole dataset was consistent with a wide mobilization of root-secreted phytase/phosphatase activities, which makes it a candidate for external phytic acid hydrolysis in maize. However, a more complex response to Po source, indicating a possible direct uptake of $InsP_6$ by maize roots, emerged from our RNA-seq data consistent with a limiting effect of maize root-secreted phytase/phosphatase activities. Finally, the leaf interveinal chlorosis in Po-treated plants of both populations (Fig. 1c) indicated a side-effect of the use of phytic acid as P source due to its chelating properties towards metal ions, thus impairing the maize chelation-based strategy of mineral uptake that can negatively affect maize shoot growth more than root [73].

Different numbers of DEGs were involved in organic P treatment response by the two maize populations

The expression changes induced by organic P treatment (Po) with respect to the mineral (Pi) control treatment involved a very different number of DEGs in the two maize populations: 58 in P1547 and 618 in VA572. The six DEGs common to both the populations, all downregulated (Fig. 3d) and four of them also downregulated in the 21DAT and/or 28DAT Po *vs* Pi comparisons, are likely to be involved in root cell wall modifications

induced by Po treatment in the last sampling times: Zm00001d002687, an ortholog of rice CYP86A11 (Os04g0560100) involved in root suberin pathway [74], Zm00001d028689, *ZmPHR1*-regulated ABC transporter, associated with the symplastic transport in the suberized cell wall [75], Zm00001d037359, a peroxidase implicated in abiotic stress response [76] and the hypothetical protein Zm00001d031822 (Tables S5 and S6).

The greatest difference between the maize populations concerned the upregulated DEGs in Po treatment, specific to each population: seven in P1547 hybrid (Zm00001d044541, Zm00001d052112, Zm00001d017429, Zm00001d042062, Zm00001d041352 in Table 1, the MATE transporter Zm00001d004055 and the hypothetical protein Zm00001d042030) and 503 in VA572 populations, 28 among which present in Table 1. Then, in term of number of genes positively induced by Po treatment, VA572 showed an increased expression plasticity with respect to the P1547 hybrid. However, among the 178 genes common to VPo *vs* VPi and HPi *vs* VPi comparisons (Fig. 3b) 140 resulted upregulated in both the comparisons indicating that about 28% of the Po-induced genes in VA572 had a higher constitutive (baseline) expression in P1547 hybrid than in VA572 in the "control" situation represented by the Pi treatment. Seven DEGs in Table 1 were consistent with this situation. Higher constitutive expression in P1547 hybrid, possibly derived from heterosis exploitation specific to the F1 hybrid variety model, could provide an effective way to face the environmental change represented by Po treatment consistent with the higher baseline strategy illustrated by Rivera et al. [77] in providing a reaction norm framework for gene expression plasticity across varying experimental conditions. On the contrary, among the 221 genes common to VPo *vs* VPi and HPo *vs* VPo comparisons (Fig. 3b), 199 resulted more expressed in VPo then HPo thus indicating that about 40% of the Po-induced genes in VA572 reacted more to Po condition than P1547 hybrid, i.e. had a greater gene expression plasticity [77]. Fourteen DEGs in Table 1 were consistent with this situation. The larger shift of transcriptomic profile in the two P treatments displayed by VA572 and the higher baseline expression with reduced expression plasticity of P1547 hybrid appear as different ways to face the environmental change of P sources likely in relation with the agronomic context of cultivation and breeding and with the variety models adopted for the two populations. A thorough investigation spanning the entire vegetative and reproductive crop stages should be necessary to know whether these different strategies can evolve towards better adapted phenotypes in organic P exploitation.

Similar responses to Po treatment were achieved via different pathways in the two maize populations

In both the populations the *ZmPHR*-mediated induction of the phosphate starvation-induced genes was inhibited in Po treatment mainly via the SPX protein (Zm00001d044541) interaction with *ZmPHR* in P1547 hybrid and likely via the downregulation of the conserved regulatory module of Pi homeostasis formed by PHR1, miR399, and PHO2 [78, 79] in VA572. These responses clearly indicated that $InsP_6$ is perceived by maize plants as an available P source. The putative PAP Zm00001d0277731, induced by Po treatment in VA572 and highly constitutively expressed in P1547 hybrid, is likely to play a role in the root-secreted enzymatic phosphate cleavage from $InsP_6$. However, the downregulation of Zm00001d046234, responsible for myo-inositol degradation into D-glucuronate [80], induced by Po treatment in VA572 suggested that a direct uptake of $InsP_6$ by maize roots could also take place. Notably, Roberts et al., [80] demonstrated that excised maize root tips were able to rapidly remove myo-inositol from the medium, using it as precursor in pectic cell wall biosynthesis. This uptake/internal transfer could be mediated by different transporters (Zm00001d044442, Zm00001d027625, Zm00001d037160, Zm00001d022636) induced by Po treatment in VA572 (Table 1 and GO 0055085 Fig. 4) while in P1547 hybrid mainly mediated by the same SPX4 proteins also interacting with *ZmPHR* and by the other *ZmSPX* gene Zm00001d029460. The introduced $InsP_6$ is likely to be partly directed to synthesis of membrane phosphoinositides (PIPs), the membrane lipids based on phosphatidylinositol, and of sphingolipids (SLs), a diversified class of lipids characterizing membrane architecture and biophysical properties [81]. PIP homeostasis is regulated by SEC14 proteins (Zm00001d053333) induced by Po treatment in VA572 and highly constitutively expressed in P1547 hybrid; PIPs have been reported to play important roles in tip-growing cells such as root hairs [82].

Maize root morphology is known to be affected by P status [55] and VA572 appeared to exert a more thorough regulation on root development in response to Po treatment than P1547 hybrid. The primary root elongation was likely inhibited by Zm00001d040035, upregulated in Po treated VA572 and highly constitutively expressed in P1547 hybrid, an opposite effect compared to low P condition [55], while similar was the upregulation of Zm00001d032732 suggesting an inhibition of lateral root development. In VA572, a modulation in root IAA and gibberellin levels in Po treatment are suggested by the upregulation of the auxin regulator genes (Zm00001d018414, Zm00001d039624, Zm00001d003311, Table 1; Zm00001d043179, GO 0055085 Fig. 4) and the

gibberellin receptor Zm00001d038165 and by the modulation of the auxin antagonistic cytokinin via the upregulation of the cytokinin oxidase Zm00001d039520 (Table 1). The induction of Zm00001d036416, a regulator of root meristem development by modulating auxin and cytokinin activities, induced by Po treatment in VA572, suggested a fine-tuned regulation of root meristem activity in VA572. A common feature of both the populations was the reduction of lignin (Zm00001d043019) and suberin (Zm00001d049020) pathways induced by Po treatment and suggesting a greater root cell wall extensibility. The TF Zm00001d052112 appeared specific to P1547 hybrid and clearly induced by Po treatment; this gene contained an auxin-responsive-related element [58] suggesting an involvement in root meristem hormonal regulation.

A modulation of Pi and NO_3 uptake under Pi starvation was found by Wang et al., [83] in *Aradidopsis* and maize. In our experimental conditions, NO_3 uptake was clearly inhibited in Po-treated P1547 hybrid via the downregulation of both the main high affinity root NO_3 transporters Zm00001d054057 and Zm00001d054060. In VA572 the NO_3 uptake inhibition appeared less important as only the low affinity transporter Zm00001d006823 was downregulated while NO_3 assimilation was enhanced via the upregulation of two nitrate reductases, one of which (Zm00001d049995) high constitutively expressed in P1547 hybrid (Table 1). Interestingly, none of the maize NH_4 transporters [61] were found among the DEGs indicating that NH_4-N, the only mineral N form present in animal effluents/digestates, should be readily available to plants.

As for K^+ transport systems, represented by potassium channels and transporters [62], Po treatment enhanced the role of K^+ channels Zm00001d003555 and Zm00001d037289, upregulated in VA572, with respect to the high affinity transporter Zm00001d003859, downregulated, probably to maintain K^+ root homeostasis by minimizing energy cost and fully exploiting the regulatory networks of K^+ channels [84, 85].

Increased carbon and energy needs were induced by Po treatment in VA572 as indicated by the upregulation of sucrose-cleaving enzymes in VPo *vs* VPi possibly to sustain the growth of maize root tips and the cost of transcription, translation, and protein turnover linked to the larger root transcriptomic changes present in this population with respect to P1547 hybrid. Phytic acid has known chelating properties of metal ions such iron (Fe) and zinc (Zn) essential for plant growth and development; a possible interference between Po treatment and metal ion uptake by maize root was put in evidence by interveinal chlorosis in young leaves (yellow stripes) of Po-treated plants of both populations (Fig. 1c). In fact both populations were affected by impairment of Fe(III) homeostasis and reacted by promoting phytosiderophore release (Zm00001d017429, Zm00001d041111, Zm00001d041352) and Fe(III)-phytosiderophore uptake (Zm00001d052435) to cope with iron deficiency, in particular at 28DAT. These widespread changes in biological processes in response to different P sources agreed with the enriched functional significance of response to stimulus and chemical stimulus and transmembrane transport evidenced by GO enriched analysis and suggest the implementation of a complex adaptation pattern in Po-treated maize plants.

Conclusions

This study indicates that phytic acid is a bioavailable P source for maize seedling growth although the entire vegetative and reproductive crop cycle should be assessed to verify this result. Both phosphate cleavage from $InsP_6$ by root-secreted PAPs and a direct uptake of myo-inositol at various degree of phosphorylation are suggested by the root RNA-seq data presented. A wider mobilization of genes/pathways and a steeper slope of the expression reaction across P treatments (expression plasticity) are induced by Po treatment in VA572 while the response pattern of P1547 hybrid is based on a higher baseline expression in Pi treatment with reduced expression plasticity across P treatments. The physiological responses to Po treatment, inferred from DEG analysis of P treatments within population comparisons, are similar in both the populations but the patterns of genes involved often differed being specific to each population.

Supplementary Information

The online version contains supplementary material available at https://doi.org/10.1186/s12870-025-06431-y.

Supplementary Material 1: Figure S1. Example of plant growing technique: experimental unit

Supplementary Material 2: Figure S2. Root and shoot P content (a) and P use efficiency PUE (b) in population x P treatment x sampling time combinations. The values are the means ± SE of the two experiments per population; different letters above bars indicate significant differences ($p<0.05$, italic; $p<0.005$, normal font) among treatments within sampling times by linear contrasts

Supplementary Material 3: Figure S3. PCR analysis on AMF 18S rRNA gene fragment in cDNA root samples of P1547 Hybrid (A) and VA572 (B) populations. Samples are bulks of four biological replicates. MK: Marker 1Kb DNA Ladder (Thermo Scientific); Positive controls: C1 (cDNA from plants of *M. truncatula* inoculated with AMF), C2 (DNA from plants of *M. truncatula* inoculated with AMF) and C3 (DNA from rice colonized by AMF). Positive controls were provided by Erica Lumini, (CNR-IPSP, Torino, Italy).

Supplementary Material 4: Figure S4. Root-associated phytase activity in the different population x P treatment x sampling time combinations. The values reported are the means ± SE of the two experiments per population; different letters above bars indicate significant differences ($p<0.05$, italic; $p<0.005$, normal font) among treatments within sampling times by with linear contrasts

Supplementary Material 5: Figure S5. Cluster analysis based on the whole dataset of 32,079 genes resulting from RNA-seq analysis

Supplementary Material 6: Table S1. List of PCR primers used in the study

Supplementary Material 7: Table S2. RNA-seq analysis: summary of the results. M: millions

Supplementary Material 8: Table S3. Analysis of variance (ANOVA) results (F value and significance). Effect of P treatments (Pi, Po, noP), sampling times (7, 14, 21, 28 DAT) and experiment on growth parameters, P concentration/content and PUE in plant tissues and root phytase activity in the maize P1547 Hybrid (A) and VA572 (B) populations

Supplementary Material 9: Table S4. List of differentially expressed genes (DEGs) in the population within P treatment comparisons (HPo *vs* VPo and HPi vs VPi).

Supplementary Material 10: Table S5. List of differentially expressed genes (DEGs) in the P treatment within population comparisons (HPo *vs* HPi and VPo *vs* VPi).

Supplementary Material 11: Table S6. List of differentially expressed genes (DEGs) in the P treatment within sampling time comparisons (14DATPo *vs* 14DATPi; 21DATPo *vs* 21DATPI; 28DATPo *vs* 28DATPi).

Supplementary Material 12: Data S1. RNA-seq analysis. Expression data of the 32,079 genes used for differential expression analysis normalized using DESeq2 package.

Supplementary Material 13: Figure S6. Expression values of 13 genes chosen for qRT PCR (y axis) vs RNAseq (x axis): plot diagram (r=0.73***)

Acknowledgements
Technical support from Annalisa Carenzi and Giuseppina Malagni (CREA - Research Centre for Animal Production and Aquaculture, Lodi, Italy) and from Giulia Bassanini (PTP Science Park, Lodi, Italy) is gratefully acknowledged. The bioinformatic support of Nelson Nazzicari (CREA - Research Centre for Animal Production and Aquaculture, Lodi, Italy) is also acknowledged. Maize seeds of VA572 used in this study were kindly provided by Paolo Stefano Valoti (CREA – Research Centre for Cereal and Industrial Crops, Bergamo, Italy).

Clinical trial number
Not applicable.

Authors' contributions
MC and CS designed the research; MC and FT performed the experiments and analyzed the data with CS. MC and CS wrote the manuscript.

Funding
This research activity has been funded by ROP ERDF 2014–2020 Lombardy – Innovation and Competitiveness.

Data availability
The data supporting the conclusions of this study are included in this published article as Additional files. All sequence reads produced in RNAseq analysis have been deposited in the NCBI SRA datasets (www.ncbi.nlm.nih.gov/sra) under the accession number PRJNA1182976.

Declarations

Ethics approval and consent to participate
Not applicable.

Consent for publication
Not applicable.

Competing interests
The authors declare no competing interests.

Received: 17 September 2024 Accepted: 19 March 2025
Published online: 03 April 2025

References

1. Reuland G, Sigurnjak I, Dekker H, Michels E, Meers E. The Potential of Digestate and the Liquid Fraction of Digestate as Chemical Fertiliser Substitutes under the RENURE Criteria. Agronomy. 2021;11:1374. https://doi.org/10.3390/agronomy11071374.
2. Garcés-Ruiz M, Calonne-Salmon M, Plouznikoff K, Misson C, Navarrete-Mier M, Cranenbrouck S, Declerck S. Dynamics of short-term phosphorus uptake by intact mycorrhizal and non-mycorrhizal maize plants grown in a circulatory semi-hydroponic cultivation system. Front Plant Sci. 2017;8:1471.
3. Richardson AE, Simpson RJ. Soil Microorganisms Mediating Phosphorus Availability. Plant Physiol. 2011;156:989–96.
4. Wang XX, Hoffland E, Feng G, Kuyper TW. Phosphate uptake from phytate due to hyphae-mediated phytase activity by arbuscular mycorrhizal maize. Front Plant Sci. 2017;8:684.
5. Karnatam KS, Chhabra G, Saini DK, Singh R, Kaur G, Praba UP, Kumar P, Goyal S, Sharma P, Ranjan R, Sandhu SK, Kumar R, Vikal Y. Genome-Wide Meta-Analysis of QTLs associated with root traits and implications for maize breeding. Int J Mol Sci. 2023;24(7):6135. https://doi.org/10.3390/ijms24076135.
6. Lambers H, Shane MW, Cramer MD, Pearse SJ, Veneklaas EJ. Root structure and functioning for efficient acquisition of phosphorus: matching morphological and physiological traits. Ann Bot. 2006;98:693–713. https://doi.org/10.1093/aob/mcl114.
7. Richardson AE, George TS, Hens M, Simpson RJ. Utilization of soil organic phosphorus by higher plants. In: Turner BL, Frossard E, Baldwin DS eds. Organic phosphorus in the environment. CABI Publishing; 2005:ISBN 0 85199 822 4.
8. Li G, Li H, Leffelaar PA, Shen J, Zhang F. Characterization of phosphorus in animal manures collected from three (dairy, swine, and broiler) farms in China. PLoS ONE. 2014;9(7): e102698. https://doi.org/10.1371/journal.pone.0102698.
9. Tuszynska A, Czerwionka K, Obarska-Pempkowiak H. Phosphorus concentration and availability in raw organic waste and post fermentation products. J Environ Manage. 2021;278: 111468. https://doi.org/10.1016/j.jenvman.2020.111468.
10. Regelink IC, Egene CE, Tack FMG, Meers E. Speciation of P in solid organic fertilisers from digestate and biowaste. Agronomy. 2021;11:2233. https://doi.org/10.3390/agronomy11112233.
11. Li M, Osaki M, Rao IM, Tadano T. Secretion of phytase from the roots of several plant species under phosphorus-deficient conditions. Plant Soil. 1997;195:161–9.
12. Asmar F. Variation in activity of root extracellular phytase between genotypes of barley. Plant Soil. 1997;195:61–4.
13. Brinch-Pedersen H, Madsen CK, Holme IB, Dionisio G. Increased understanding of the cereal phytase complement for better mineral bio-availability and resource management. J Cereal Sci. 2014;59:373–81. https://doi.org/10.1016/j.jcs.2013.10.003.
14. Miller SS, Liu J, Allan DL, Menzhuber CJ, Fedorova M, Vance CP. Molecular control of acid phosphatase secretion into the rhizosphere of proteoid roots from phosphorus-stressed white lupin. Plant Physiol. 2001;127:594–606.
15. Bozzo GG, Dunn EL, Plaxton WC. Differential synthesis of phosphate-starvation inducible purple acid phosphatase isozymes in tomato (Lycopersicon esculentum) suspension cells and seedlings. Plant Cell Environ. 2006;29:303–13.
16. Xiao K, Harrison MJ, Wang ZY. Transgenic expression of a novel M. truncatula phytase gene results in improved acquisition of organic phosphorus by Arabidopsis. Planta. 2005;222:27–36.
17. Liang CY, Tian J, Lam HM, Lim BL, Yan XL, Liao H. Biochemical and molecular characterization of PvPAP3, a novel purple acid phosphatase isolated from common bean enhancing extracellular ATP utilization. Plant Physiol. 2010;152:854–65.
18. Lung SC, Leung A, Kuang R, Wang Y, Leung P, Lim BL. Phytase activity in tobacco (*Nicotiana tabacum*) root exudates is exhibited by a purple acid phosphatase. Phytochemistry. 2008;69:365–73.
19. Robinson WD, Park J, Tran HT, Del Vecchio HA, et al. The secreted purple acid phosphatase isozymes AtPAP12 and AtPAP26 play a pivotal role in extracellular phosphate-scavenging by Arabidopsis thaliana. J Exp Bot. 2012;63:6531–42. https://doi.org/10.1093/jxb/ers309.

20. Li C, Gui S, Yang T, Walk T, Wang X, Liao H. Identification of soybean purple acid phosphatase genes and their expression responses to phosphorus availability and symbiosis. Ann Bot. 2012;109:275–85. https://doi.org/10.1093/aob/mcr246.
21. Tian J, Wang C, Zhang Q, He X, Whelan J, Shou H. Overexpression of *OsPAP10a*, A Root-Associated Acid Phosphatase. Increased Extracellular Organic Phosphorus Utilization in Rice. 2012. https://doi.org/10.1111/j.1744-7909.2012.01143.x.
22. Kavka M, Majcherczyk A, Kües U, Polle A. Phylogeny, tissue-specific expression, and activities of root-secreted purple acid phosphatases for P uptake from ATP in P starved poplar. Plant Sci. 2021;110906:ISSN 0168-9452. https://doi.org/10.1016/j.plantsci.2021.110906.
23. Carelli M, Cabassi G, Abbruscato P, Losini I, Aggiato MS, Biazzi E, Scotti C. Different efficiencies in organic P exploitation of two Italian alfalfa (*Medicago sativa*) landraces involving a possible adaptation pattern of the phytase encoding Ms PHY1 gene. Plant Breeding. 2020;139:834–44. https://doi.org/10.1111/pbr.12833.
24. Hasan MM, Hasan MM, Teixeira da Silva JA *et al.* Regulation of phosphorus uptake and utilization: transitioning from current knowledge to practical strategies. Cell Mol Biol Lett. 2016. https://doi.org/10.1186/s11658-016-0008-y.
25. Torres-Rodríguez JV, Salazar-Vidal MN, Chávez Montes RA, Massange-Sánchez JA, Gillmor CS, Sawers RJH. Low nitrogen availability inhibits the phosphorus starvation response in maize (Zea mays ssp. mays L.). BMC Plant Biol. 2021;21(1):259. https://doi.org/10.1186/s12870-021-02997-5.
26. Ma X, Li H, Zhang J, Shen J. Spatiotemporal pattern of acid phosphatase activity in soils cultivated with maize sensing to phosphorus-rich patches. Front Plant Sci. 2021;12: 650436. https://doi.org/10.3389/fpls.2021.650436.
27. Lopes E, Silva L, Andrade JADC, Maltoni KL, Lannes LS. Potential of root acid phosphatase activity to reduce phosphorus fertilization in maize cultivated in Brazil. PLoS ONE. 2023;18(10): e0292542. https://doi.org/10.1371/journal.pone.0292542.
28. Santoro V, Della Lucia MC, Francioso O, Stevanato P, Bertoldo G, Borella M, Ferrari E, Zaccone C, Schiavon M, Pizzeghello D, et al. Phosphorus acquisition efficiency and transcriptomic changes in maize plants treated with two lignohumates. Plants. 2023;12:3291. https://doi.org/10.3390/plants12183291.
29. González-Muñoz E, Avendaño-Vázquez AO, Chávez Montes RA, de Folter S, Andrés-Hernández L, Abreu-Goodger C, Sawers RJH. The maize (Zea mays ssp. mays var. B73) genome encodes 33 members of the purple acid phosphatase family. Front Plant Sci. 2015;6:341. https://doi.org/10.3389/fpls.2015.00341.
30. Murphy J, Riley JP. A modified single solution method for the determination of phosphate in natural waters. Anal Chim Acta. 1962;27:31–6.
31. Roberts TL, Johnston AE. Phosphorus use efficiency and management in agriculture. Resour Conserv Recycl. 2015;105:275–81.
32. Lumini E, Orgiazzi A, Borriello R, Bonfante P, Bianciotto V. Disclosing arbuscular mycorrhizal fungal biodiversity in soil through a land-use gradient using a pyrosequencing approach. Environ Microbiol. 2010;12:2165–79.
33. Richardson E, Hadobas PA, Hayes JE. Acid phosphomonoesterase and phytase activities of wheat (Triticum aestivum L.) roots and utilization of organic phosphorus substrates by seedlings grown in sterile culture. Plant Cell Environ. 2000;23:397–405.
34. Del Fabbro C, Scalabrin S, Morgante M, Giorgi FM. An extensive evaluation of read trimming effects on Illumina NGS data analysis. PLoS ONE. 2013;8: e85024.
35. Woodhouse MR, Cannon EK, Portwood JL, Harper LC, Gardiner JM, Schaeffer ML, Andorf CM. A pan-genomic approach to genome databases using maize as a model system. BMC Plant Biol. 2021;21:385. https://doi.org/10.1186/s12870-021-03173-5.
36. Dobin A, Davis CA, Schlesinger F, Drenkow J, Zaleski C, Jha S, Batut P, Chaisson M, Gingeras TR. STAR: ultrafast universal RNA-seq aligner. Bioinformatics. 2013;29:15–21.
37. Wang L, Wang S, Li W. RSeQC: quality control of RNA-seq experiments. Bioinformatics. 2012;28:2184–5.
38. Anders S, Huber W. Differential expression analysis for sequence count data. Genome Biol. 2010;11:106.
39. Love MI, Huber W, Anders S. Moderated estimation of fold change and dispersion for RNA-seq data with DESeq2. Genome Biol. 2014;15:550.
40. Thomas PD, Ebert D, Muruganujan A, Mushayahama T, Albou LP, Mi H. PANTHER: Making genome-scale phylogenetics accessible to all. Protein Sci. 2022;31:8–22. https://doi.org/10.1002/pro.4218.
41. Ashburner, et al. Gene ontology: tool for the unification of biology. Nat Genet. 2000;25:25–9. https://doi.org/10.1038/75556.
42. The Gene Ontology Consortium. The Gene Ontology knowledgebase in 2023. Genetics. 2023;224:iyad031. https://doi.org/10.1093/genetics/iyad031.
43. Pei L, Liu J, Zhou Y, Jiang Y, Li H. Transcriptomic and metabolomic profiling reveals the protective role of anthocyanins in alleviating low phosphate stress in maize. Physiol Mol Biol Plants. 2021;27:889–905. https://doi.org/10.1007/s12298-021-00981-9.
44. Maugenest S, Martinez I, Godin B, Perez P, Lescure AM. Structure of two maize phytase genes and their spatio-temporal expression during seedling development. Plant Mol Biol. 1999;39:503–14.
45. Calderón-Vázquez C, Sawers RJH, Herrera-Estrella L. Phosphate Deprivation in Maize: Genetics and Genomics. Plant Physiol. 2011;156:1067–77.
46. Xu Y, Liu F, Han G, Cheng B. Genome-wide identification and comparative analysis of phosphate starvation-responsive transcription factors in maize and three other gramineous plants. Plant Cell Rep. 2018;37(5):711–26. https://doi.org/10.1007/s00299-018-2262-0.
47. Jung JY, Ried MK, Hothorn M, Poirier Y. Control of plant phosphate homeostasis by inositol pyrophosphates and the SPX domain. Curr Opin Biotechnol. 2018;49:156–62. https://doi.org/10.1016/j.copbio.2017.08.012.
48. Xiao J, Xie X, Li C, Xing G, Cheng K, Li H, Liu N, Tan J, Zheng W. Identification of SPX family genes in the maize genome and their expression under different phosphate regimes. Plant Physiol Biochem. 2021;168:211–20. https://doi.org/10.1016/j.plaphy.2021.09.045.
49. Liu F, Xu Y, Jiang H, Jiang C, Du Y, Gong C, Wang W, Zhu S, Han G, Cheng B. systematic identification, evolution and expression analysis of the *Zea mays* PHT1 gene family reveals several new members involved in root colonization by arbuscular mycorrhizal fungi. Int J Mol Sci. 2016;17:930. https://doi.org/10.3390/ijms17060930.
50. Kumar K, Yadava P, Gupta M, Choudhary M, Jha AK, Wani SH, Dar ZA, Kumar B, Rakshit S. Narrowing down molecular targets for improving phosphorus-use efficiency in maize (Zea mays L.). Mol Biol Rep. 2022;49:12091–107. https://doi.org/10.1007/s11033-022-07679-5.
51. Zhang S, Yang W, Zhao Q, Zhou X, Jiang L, Ma S, Liu X, Li Y, Zhang C, Fan Y, Chen R. Analysis of weighted co-regulatory networks in maize provides insights into new genes and regulatory mechanisms related to inositol phosphate metabolism. BMC Genomics. 2016;17:129. https://doi.org/10.1186/s12864-016-2476-x.
52. Pilu SR, Panzeri D, Gavazzi G, Rasmussen S, Consonni G, Nielsen E. Phenotypic, genetic and molecular characterization of a maize low phytic acid mutant (lpa241). Theor Appl Genet. 2003;107:980–7.
53. Linn J, Ren M, Berkowitz O, Ding W, van der Merwe MJ, Whelan J, Jost R. Root cell-specific regulators of phosphate-dependent growth. Plant Physiol. 2017;174(3):1969–89. https://doi.org/10.1104/pp.16.01698.
54. De Campos MKF, Schaaf G. The regulation of cell polarity by lipid transfer proteins of the SEC14 family. Curr Opin Plant Biol. 2017;40:158–68. https://doi.org/10.1016/j.pbi.2017.09.007.
55. Zhang X, Wang B, Zhao Y, Zhang J, Li Z. Auxin and GA signaling play important roles in the maize response to phosphate deficiency. Plant Sci. 2019;283:177–88. https://doi.org/10.1016/j.plantsci.2019.02.011.
56. McReynolds MR, Dash L, Montes C, Draves MA, Lang MG, Walley JW, Kelley DR. Temporal and spatial auxin responsive networks in maize primary roots. Quant Plant Biol. 2022;3: e21. https://doi.org/10.1017/qpb.2022.17.
57. Zheng Z, Hey S, Jubery T, Liu H, Yang Y, Coffey L, Miao C, Sigmon B, Schnable JC, Hochholdinger F, Ganapathysubramanian B, Schnable PS. Shared Genetic Control of Root System Architecture between *Zea mays* and *Sorghum bicolor*. Plant Physiol. 2020;182(2):977–91. https://doi.org/10.1104/pp.19.00752.
58. Qin L, Chen H, Wu Q, Wang X. Identification and exploration of the GRF and GIF families in maize and foxtail millet. Physiol Mol Biol Plants. 2022;28:1717–35. https://doi.org/10.1007/s12298-022-01234-z.
59. Tang Y, Liu H, Guo S, Wang B, Li Z, Chong K, Xu Y. OsmiR396d affects gibberellin and brassinosteroid signaling to regulate plant architecture in rice. Plant Physiol. 2018;176(1):946–59. https://doi.org/10.1104/pp.17.00964.
60. Jia L, Hu D, Wang J, Liang Y, Li F, Wang Y, Han Y. Genome-Wide identification and functional analysis of nitrate transporter genes (NPF, NRT2 and NRT3) in maize. Int J Mol Sci. 2023;24(16):12941. https://doi.org/10.3390/ijms241612941.

61. Dechorgnat J, Francis KL, Dhugga KS, Rafalski JA, Tyerman SD, Kaiser BN. Tissue and nitrogen-linked expression profiles of ammonium and nitrate transporters in maize. BMC Plant Biol. 2019;19(1):206. https://doi.org/10.1186/s12870-019-1768-0.
62. Zhang Z, Zhang J, Chen Y, Li R, Wang H, Wei J. Genome-wide analysis and identification of HAK potassium transporter gene family in maize (Zea mays L.). Mol Biol Rep. 2012;39(8):8465–73. https://doi.org/10.1007/s11033-012-1700-2.
63. Li T, Yang H, Lu Y, Dong Q, Liu G, Chen F, Zhou Y. Comparative transcriptome analysis of differentially expressed genes related to the physiological changes of yellow-green leaf mutant of maize. Peer J. 2021;9: e10567. https://doi.org/10.7717/peerj.10567.
64. Schaaf G, Ludewig U, Erenoglu BE, Mori S, Kitahara T, von Wirén N. ZmYS1 functions as a proton-coupled symporter for phytosiderophore- and nicotianamine-chelated metals. J Biol Chem. 2004;279(10):9091–6. https://doi.org/10.1074/jbc.M311799200.
65. Ogo Y, Itai RN, Nakanishi H, Inoue H, Kobayashi T, Suzuki M, Takahashi M, Mori S, Nishizawa NK. Isolation and characterization of IRO2, a novel iron-regulated bHLH transcription factor in graminaceous plants. J Exp Bot. 2006;57:2867–78. https://doi.org/10.1093/jxb/erl054.
66. Nozoye T, Nakanishi H, Nishizawa NK. Characterizing the crucial components of iron homeostasis in the maize mutants ys1 and ys3. PLoS ONE. 2013;8(5): e62567. https://doi.org/10.1371/journal.pone.0062567.
67. Tian MZ, Wang HF, Tian Y, Hao J, Guo HL, Chen LM, Wei YK, Zhan SH, Yu HT, Chen YF. ZmPHR1 contributes to drought resistance by modulating phosphate homeostasis in maize. Plant Biotechnol J. 2024;22:3085–98. https://doi.org/10.1111/pbi.14431.
68. Wang X, Feng J, White PJ, Shen J, Cheng L. Heterogeneous phosphate supply influences maize lateral root proliferation by regulating auxin redistribution. Ann Bot. 2020;125(1):119–30. https://doi.org/10.1093/aob/mcz154.
69. Tarafdar JC, Claassen N. Organic phosphorus compounds as a phosphorus source for higher plants through the activity of phosphatases produced by plant roots and microorganisms. Biol Fertil Soils. 1988;5:308–12.
70. Hayes JE, Simpson RJ, Richardson AE. The growth and phosphorus utilisation of plants in sterile media when supplied with inositol hexaphosphate, glucose 1-phosphate or inorganic phosphate. Plant and Soil. 2000;220:165–74.
71. Lung SC, Lim BL. Assimilation of phytate-phosphorus by extracellular phytase activity of *tobacco* (*Nicotiana tobaccum*) is affected by the availability of soluble phytate. Plant Soil. 2006;279:187–99.
72. Findenegg GR, Nelemans JA. The effect of phytase on the availability of P from myo-inositol exaphosphate (phytate) for maize roots. Plant Soil. 1993;154:189–96.
73. Xu J, Qin X, Zhu H, Chen F, Fu X, Yu F. Mapping of the Quantitative Trait Loci and candidate genes associated with iron efficiency in maize. Front Plant Sci. 2022;13: 855572. https://doi.org/10.3389/fpls.2022.855572.
74. Colmer TD, Kotula L, Malik AI, Takahashi H, Konnerup D, Nakazono N, Pedersen O. Rice acclimation to soil flooding: Low concentrations of organic acids can trigger a barrier to radial oxygen loss in roots. Plant Cell Environ. 2019;42:2183–97. https://doi.org/10.1111/pce.13562.
75. Gao P, Wang P, Du B, et al. Accelerated remodeling of the mesophyll-bundle sheath interface in the maize C4 cycle mutant leaves. Sci Rep. 2022;12:5057. https://doi.org/10.1038/s41598-022-09135-7.
76. Wang Y, Wang Q, Zhao Y, Han G, Zhu S. Systematic analysis of maize class III peroxidase gene family reveals a conserved subfamily involved in abiotic stress response. Gene. 2015;566(1):95–108. https://doi.org/10.1016/j.gene.2015.04.041.
77. Rivera HE, Aichelman HE, Fifer JE, Kriefall NG, Wuitchik DM, Wuitchik SJS, Davies SW. A framework for understanding gene expression plasticity and its influence on stress tolerance. Mol Ecol. 2021;30(6):1381–97. https://doi.org/10.1111/mec.15820.
78. Bari R, Datt Pant B, Stitt M, Scheible WR. PHO2, microRNA399, and PHR1 define a phosphate-signaling pathway in plants. Plant Physiol. 2006;141(3):988–99. https://doi.org/10.1104/pp.106.079707.
79. Wang X, Yuan D, Liu Y, Liang Y, He J, Yang X, Hang R, Jia H, Mo B, Tian F, Chen X, Liu L. INDETERMINATE1 autonomously regulates phosphate homeostasis upstream of the miR399-ZmPHO2 signaling module in maize. Plant Cell. 2023;35(6):2208–31. https://doi.org/10.1093/plcell/koad089.
80. Roberts RM, Deshusses J, Loewus F. Inositol metabolism in plants. V. Conversion of myo-inositol to uronic acid and pentose units of acidic polysaccharides in root-tips of Zea mays. Plant Physiol. 1968;43:979–89.
81. Cassim AM, Grison M, Ito Y, Simon-Plas F, Mongrand S, Boutté Y. Sphingolipids in plants: a guidebook on their function in membrane architecture, cellular processes, and environmental or developmental responses. FEBS Lett. 2020;594:3719–38.
82. Vincent P, Chua M, Nogue F, Fairbrother A, Mekeel H, Xu Y, Allen N, Bibikova TN, Gilroy S, Bankaitis VA. A Sec14p-nodulin domain phosphatidylinositol transfer protein polarizes membrane growth of Arabidopsis thaliana root hairs. J Cell Biol. 2005;168:801–12. https://doi.org/10.1083/jcb.200412074.
83. Wang X, Wang HF, Chen Y, Sun MM, Wang Y, Chen YF. The transcription factor NIGT1.2 modulates both phosphate uptake and nitrate influx during phosphate starvation in arabidopsis and maize. Plant Cell. 2020;32(11):3519–34. https://doi.org/10.1105/tpc.20.00361.
84. Guo S, Liu Z, Sheng H, Olukayode T, Zhou Z, Liu Y, Wang M, He M, Kochian L, Qin Y. Dynamic transcriptome analysis unravels key regulatory genes of maize root growth and development in response to potassium deficiency. Planta. 2023;258(5):99. https://doi.org/10.1007/s00425-023-04260-7.
85. Mallikarjuna MG, Tomar R, Lohithaswa HC, Sahu S, Mishra DC, Rao AR, Chinnusamy V. Genome-wide identification of potassium channels in maize showed evolutionary patterns and variable functional responses to abiotic stresses. Plant Physiol Biochem. 2023. https://doi.org/10.1016/j.plaphy.2023.108235.

Publisher's Note